



## Investigation of the earthquake (Michoacan-Colima) in Mexica (19.09.2022) by using GNSS stations and INSAR observations

*Atunç Pırtı\*, Mehmet Ali Yücel*

Pırtı, A., Yücel, M.A. 2024. Investigation of the earthquake (Michoacan-Colima) in Mexica (19. 09. 2022) by using GNSS stations and INSAR observations. *Baltica* 37 (2),170–179. Vilnius. ISSN 1648-858X.

Manuscript submitted 27 May 2024 / Accepted 6 November 2024 / Available online 12 December 2024

© Baltica 2024

**Abstract.** The North American Plate is subducted under the Cocos and Rivera plates, while the Pacific Plate divides from the North American Plate near the spreading centre of the Baja California Gulf, placing the Mexican Republic in a seismically active area of the world. The earthquake of a magnitude of  $M_w$  7.6–7.7 occurred 37 km southeast of the town of Aquila (near the municipality of Coalcoman) at a depth of 15.1 km on 19.09.2022 at 18:05:06 UTC (13:05:06 local time (LT)). This study focuses on the use of GNSS (Global Navigation Satellite System) data to investigate the Mexican earthquake, and the results (using static-kinematic methods) are presented in this paper. The TNCC and COL2 IGS stations, which are situated to the north and northwest of the fault, recorded the largest displacements after GNSS data processing. At five points, 9–25 cm horizontal motions were obtained in the southwest, northwest, and west directions. The quantity of horizontal motions, however, was smaller in the south of the fault stations UCOE (approximately 9–10 cm) and PENA (about 9 cm). A comparison between the GNSS and InSAR (Interferometric Synthetic Aperture Radar) results from the COMET-LiCSAR analysis showed that the GNSS and InSAR solution mirrors the pattern of earthquakes. The GNSS and InSAR data were aligned by standardizing to a common spatial and temporal grid, with corrections for atmospheric delays and noise. The mirroring of patterns was evaluated by using correlation analysis, displacement magnitude comparison, and assessment of spatial gradients. Error tolerances were considered to validate the alignment and highlight any discrepancies.

*Keywords:* 2022 Mexican earthquake; IGS stations; deformation; accuracy; motion

✉ *Atunç Pırtı\** ([atinc@yildiz.edu.tr](mailto:atinc@yildiz.edu.tr)),  <http://orcid.org/0000-0001-9197-3411>;

*Department of Geomatic Engineering, Yıldız Technical University, 34220 Esenler, Istanbul, Türkiye;*

*Mehmet Ali Yücel* ([aliyucel@comu.edu.tr](mailto:aliyucel@comu.edu.tr)),  <https://orcid.org/0000-0001-6956-5219>;

*Department of Geomatics Engineering, Canakkale Onsekiz Mart University, 17100 Canakkale, Türkiye*

*\*Corresponding author*

## INTRODUCTION

The Cocos and Rivera plates subduct under the North American Plate, while the Pacific Plate splits from the North American Plate in the Baja California Gulf spreading centre, putting the Mexican Republic in a very seismic area of the world. In addition, the Trans-Mexican Volcanic Belt, a component of the Pacific Ring of Fire, passes across the nation. There have been several earthquakes, but the one that struck on 19 September 1985 had the highest mag-

nitude. Mexico is located in two earthquake-prone regions. Southern Mexico is located slightly north of the border between the Cocos and Rivera tectonic plates and the North American Tectonic Plate, whereas the Baja California Peninsula is close to the barrier between the North American Tectonic Plate and the Pacific Plate. While the Pacific and Rivera plates are migrating northwest with respect to the North American Plate, the Cocos plate is subducting beneath the North American Tectonic Plate at a pace of 67 millimetres per year. Additionally, there

are several faults in southern Mexico, which contributes to the region's strong tectonic activity. Though not as seismically active as the region at the border between the North American and Cocos plates, north-eastern Mexico and the Yucatan Peninsula are nonetheless susceptible to severe earthquakes. An earthquake with a moment magnitude of 7.6–7.7 occurred on 19 September 2022, at 13:05:06 local time, between the Mexican states of Michoacán and Colima. The greatest intensity of the earthquake, which had a depth of 15.1 kilometres, was VIII (Severe) on the Modified Mercalli intensity scale. According to the USGS, the epicentre was located close to the municipality of Coalcomán, 37 kilometres southeast of the town of Aguila. Over the course of many states, two individuals were killed and at least 35 more were injured. On 22 September, a magnitude 6.8 aftershock occurred, adding three additional fatalities. This little earthquake struck a seismically active area close to the central Mexican coast. The earthquake occurred close to the intersection of three tectonic plates: the Cocos Plate to the south, the Rivera Plate to the northwest, and the North American Plate to the northeast. Under the North American Plate, the Rivera Plate and the Cocos Plate are both being subducted. Compared to the North American Plate, the Cocos Plate is migrating northwest at a pace of around 4.5 centimetres per year, while the slower Rivera Plate is subducting at a rate of about 2 centimetres (0.79 in) per year. On the tectonic divide between the Cocos Plate and the North American Plate, thrust faulting caused the earthquake to happen. It was near to earthquakes of 1985, 1995, and 2003 that this one struck. According to the United States Geological Survey, earthquakes of this magnitude generally rupture across a 90 km by 40 km region. A lot of studies were performed about the Mexican earthquake (Arambula-Mendoza *et al.* 2018; Arroyo *et al.* 2010; Galvis *et al.* 2020; Rodríguez-Pérez *et al.* 2020; Escobar 2003; Garcia-Acosta 2001; Zúñiga *et al.* 2000). In this work, we focused on analysing the movements of five points near the earthquake zone at the time of the earthquake. The GNSS (Global Navigation Satellite System) and InSAR (Interferometric Synthetic Aperture Radar) are powerful tools for seismic investigation in tectonically active zones like Mexico due to their ability to precisely measure ground deformation. The GNSS provides continuous, high-precision data on land movement in real-time, which is crucial for tracking gradual shifts and sudden displacements along fault lines. The InSAR, on the other hand, captures broad-area displacement patterns with high spatial resolution, making it valuable for mapping deformation over extensive regions affected by seismic events. Together, they offer complementary insights – GNSS for detailed tempo-

ral monitoring and InSAR for spatial coverage – enhancing our understanding of complex tectonic processes in active seismic areas.

## MATERIALS AND METHODS

The GNSS data were used to measure the minor ground displacements occurring between earthquakes. Static and kinematic methods were applied to evaluate GNSS data. Static GNSS surveys deliver the highest-accuracy positions available in a system, as they occupy a point for longer periods than kinematic systems. Static systems include a range of survey styles, from rapid static surveys to continuously operating stations, such as CORS sites. Kinematic GNSS surveys, on the other hand, are used to rapidly collect large numbers of high-precision survey positions, which are post-processed against a static base station. The system consists of a base station, a rover, and potentially a radio system. The basis of the kinematic system is a mobile rover, which takes initial positions, and a base station, which allows for corrections to the rover's position. The rover is carried to each measurement site and stabilized during a short occupation, typically 5–30 seconds, to acquire an initial position. The rover's position is processed against the static base station's position to remove several types of error, including integer ambiguity and atmospheric delays, resulting in a high-precision position for the rover on the order of several centimetres (Erkoç, Doğan 2023). Displacement values were computed by subtracting the kinematic results from the static results (Pırtı *et al.* 2023). On 19 September 2022, at 18:05:06 UTC, a 7.6-magnitude earthquake struck the Mexican state of Michoacán. On 22 September, at 06:16:09 UTC, a nearby 6.8-magnitude aftershock was recorded. These events took place within the scope of the Network of the Americas (NOTA), a network of permanent GPS/GNSS stations and borehole instrumentation run by the University NAVSTAR Consortium (UNAVCO) and IGS for various purposes, including monitoring plate motion and transient deformation. Through a partnership between TLALOCNet and Universidad Nacional Autónoma de México (UNAM), data from stations close to the event, as provided by UNAVCO, were utilized in this study. The UNAVCO operates the Geodetic Facility for the Advancement of Geoscience (GAGE) Facility with support from the National Science Foundation (NSF) and the National Aeronautics and Space Administration (NASA) under NSF Cooperative Agreement EAR-1724794, which is the source of these data. A crucial component of the NSF GAGE Facility is NOTA.

The GNSS and InSAR data comparison involved several key steps to ensure accurate alignment and

pattern verification (Erkoç *et al.* 2022). First, the GNSS displacement measurements were temporally aligned with the InSAR acquisition dates to establish a common temporal reference frame. Spatial alignment was achieved by using precisely located GNSS stations as ground control points for the InSAR data. The comparison criteria focused on three main aspects: (1) the magnitude of displacement vectors, (2) the directional components of movement, and (3) the temporal evolution of deformation patterns. A statistical correlation analysis was performed between GNSS-derived displacements and InSAR-derived displacement fields within a 100-meter radius of each GNSS station. Pattern “mirroring” was quantitatively assessed using a cross-correlation coefficient threshold of 0.85, with particular attention paid to areas showing significant deformation signals in both datasets. This integrated approach allowed for a robust validation of the observed deformation patterns across different spatial and temporal scales.

### Study site

Mexico is located in two regions with significant earthquake activity. While southern Mexico is located just to the north of the line separating the North American Plate from the Cocos and Rivera tectonic plates, the Baja California Peninsula is located close to the line separating the Pacific Plate and the North American Plate. At a motion of 67 mm (0.220 ft) each year, the Cocos Plate is subducting under the North American Plate, while the Pacific and Rivera plates are migrating northwest with respect to the North American Plate. Additionally, the region of southern Mexico experiences tremendous tectonic activity due to the abundance of faults there (Fig. 1). Although the Yucatan Peninsula and north-eastern Mexico do not have as much seismic activity as the region along the border between the North American and Cocos plates, damaging earthquakes may nevertheless happen there (Escobar 2003; García-Acosta 2001).

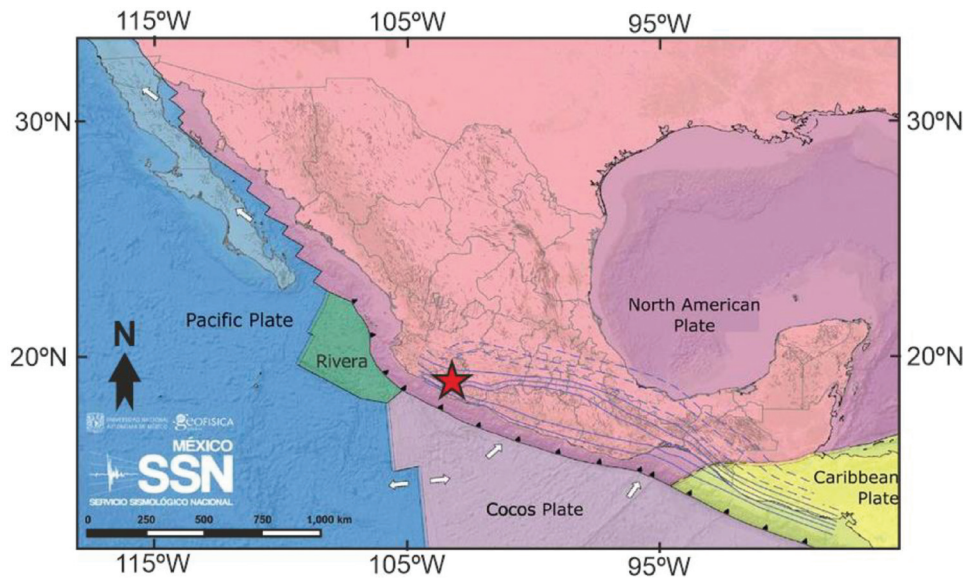


Fig. 1 The Mexican fault zone, epicentre of the earthquake, Michoacán, Mexico; Mw 7.6–7.7 earthquake

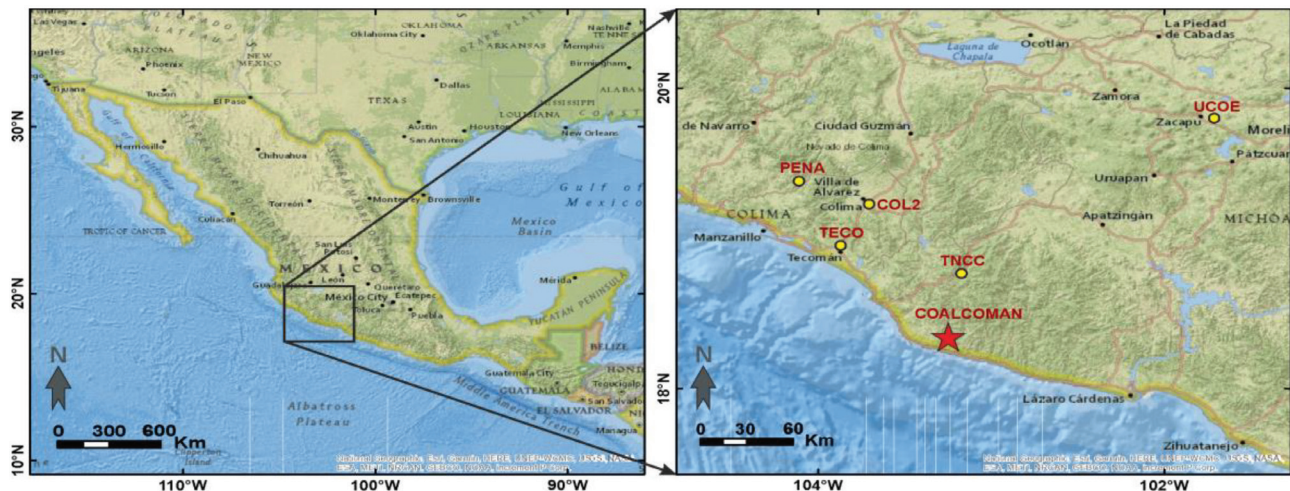


Fig. 2 Five IGS and UNAVCO stations in the study region



## RESULTS

### GNSS Surveys

The Michoacán, Mexico earthquake's displacement will be essential to revealing earthquake kinematics as a consequence, comprehending the tectonic mechanisms at play. In this case, information from five IGS and UNAVCO GNSS stations obtained close to the earthquake epicentre is quite suitable (Figs 1 and 2). To find crustal deformations, the

reference point of the system, which is downloaded at a 30-second interval, is quite helpful. In this research, data from five GNSS stations close to the epicentre of the Michoacán and Colima earthquakes were collected and analysed (see Fig. 2 and Table 1). The displacements associated with earthquakes were determined by analysing time series generated continuously (19 September 2022) by GNSS solutions (Figs 3 and 4). Table 2 lists the five IGS and UNAVCO stations' coordinates and standard deviations (Pirtvi *et al.* 2023).

**Table 1** The earthquake's magnitude distribution on 19 September 2022 in Michoacán, Mexico

Date-Time	Latitude	Longitude	Depth (km)	Mw	Explanations
09.2022 13:05:06	18°.367 N	103°.252 W	15.10	7.6–7.7	between the Mexican states of Michoacán and Colima

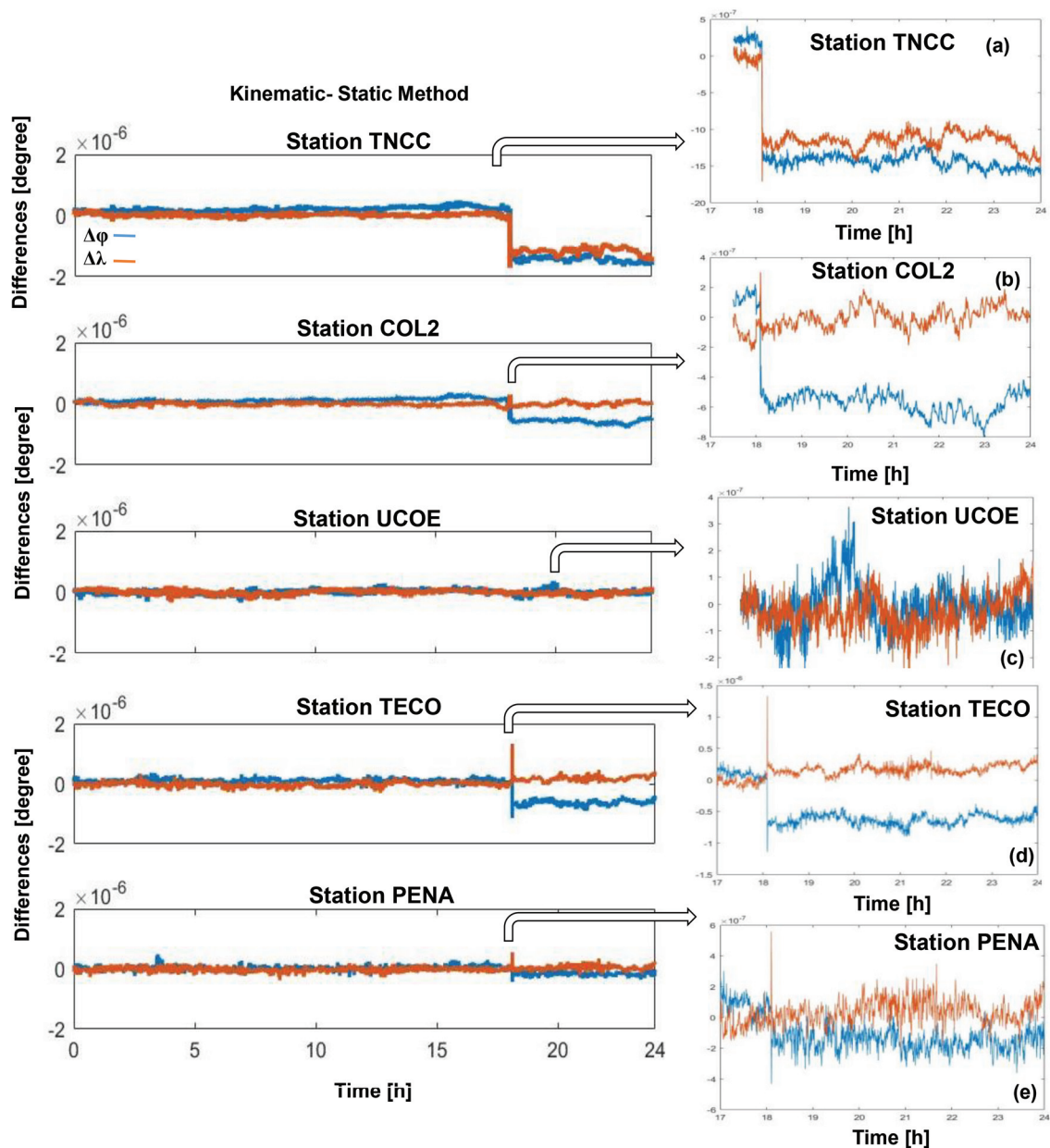


**Fig. 3** Geographic coordinates (latitude ( $\phi$ ) and longitude ( $\lambda$ )) time series (measurement period: 30 secs) acquired from five IGS and UNAVCO stations (TNCC, COL2, UCOE, TECO, and PENA) monitoring Mexican earthquake period (18:05:06 UTC Time) – (13:05:06 local time (LT)): (a) TNCC, (b) COL2, (c) UCOE, (d) TECO, (e) PENA

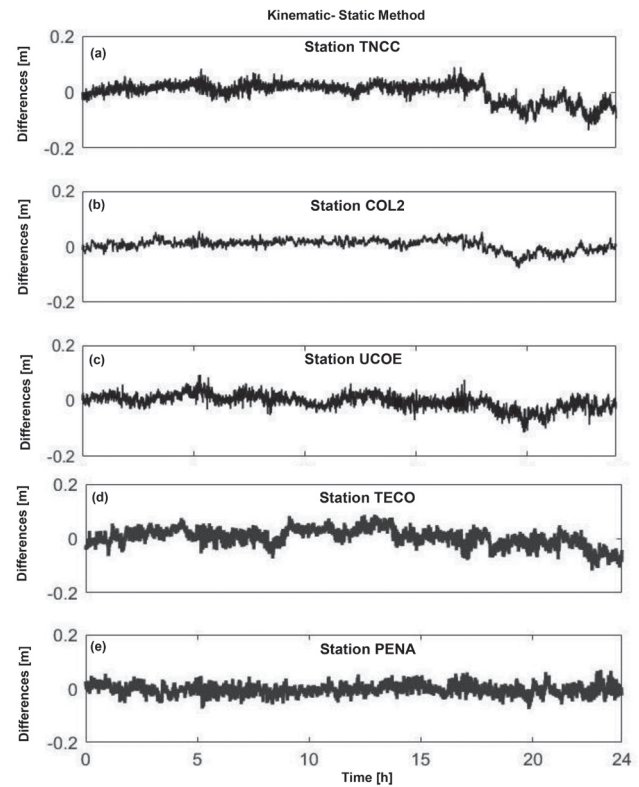
As mentioned in the previous section, five IGS and UNAVCO stations (COL2, TNCC, UCOE, TECO, and PENA) from the IGS and UNAVCO network were used in this study (Fig. 2). On 19 September 2022, these data were analysed to better understand the earthquake impacts that were evident in the time series (co-seismic displacement) (11:30:00–12:30:00 UTC Time, Fig. 3 (a), (b), (c), (d) and (e)). During this time period, the IGS and UNAVCO servers transmitted 1 hour of RINEX measurement records at 30 secs intervals to the receiver independence exchange (RINEX). The RINEX observation files (19. 09. 2022) from five IGS and UNAVCO stations were analysed using the CSRS-PPP software (kinematic and static processes, measuring period: 30 secs), as well as the kinematic approach (11:30–12:30 UTC time-measurement period: 30 secs). Five stations' ITRF 2014 epoch is 2022. Seven coordinates were collected utilizing static and kinematic processing methods (24 hours). The standard deviations of coordinate values were computed with an accuracy of 2–3 mm in the horizontal and 9–11 mm in the vertical components (Pirtti *et al.* 2023).

Figure 3 shows time series for the horizontal directions (latitude ( $\phi$ ) and longitude ( $\lambda$ ) coordinates) from the COL2, TNCC, UCOE, TECO, and PENA locations, where substantial displacement is acquired because of their adjacent location to the earthquake centre. For us to discover the displacement values, the earthquake's epicentre time is crucial. When the kinematic method is used, the receivers are either in regular motion or in constant motion. On the other hand, static methods are often more accurate and redundant than kinematic methods.

Through all these measurements, which range between several millimetres to 25 cm, the horizontal coordinate discrepancies of five stations (between static and kinematic methods) are identified (Fig. 3). The height component was also different between static and kinematic data at five stations by up to 6–8 cm, as shown in Fig. 4. With variations ranging from 9 cm to 25 cm at TNCC, COL2, UCOE, TECO, and PENA stations, Fig. 3 shows that the latitude and longitude components exhibit substantial levels through the earthquake (18:05:06 UTC time). It was possible to determine the co-seismic displacements by analysing the coordinates of five IGS and UNAVCO stations before

and after the Michoacán earthquake (19 September 2022 – Day of the Year 304). Where  $\Delta\phi_{\text{cos}}$ ,  $\Delta\lambda_{\text{cos}}$ , and  $\Delta h_{\text{cos}}$  are the co-seismic displacements,  $\phi_{\text{post}}$ ,  $\lambda_{\text{post}}$ ,  $h_{\text{post}}$ ,  $\phi_{\text{pre}}$ ,  $\lambda_{\text{pre}}$ , and  $h_{\text{pre}}$  point out the mean GNSS locations calculated from prior to and following the earthquake. Figure 5 depicts co-seismic deformation data collected for five locations based on the processes. The TNCC, TECO, and COL2 stations have larger horizontal displacement directions than the other locations, according to the GNSS surveys (Pirtti *et al.* 2023).

The movement that happened at the TNCC station during the earthquake period was found to be in the southwest direction (Fig. 5(a)). At the same time frame, it was calculated that the displacement at the COL2 station was in the direction of the west, Fig. 5(b). The UCOE point moved in all directions throughout this time, as shown in Fig. 5(c). At the TECO station, at this time, the movement was in a westward and



**Fig. 4** Vertical coordinate (exclude  $\phi$  and  $\lambda$ ) time series data derived for five IGS and UNAVCO points monitoring Mexican earthquake period: (a) TNCC, (b) COL2, (c) UCOE, (d) TECO, (e) PENA

**Table 2** The locations and standard deviations of five IGS and UNAVCO points near the earthquake region of Michoacán, Mexico (ITRF 2014 Epoch 2022.7)

Station	$\phi_{\text{ITRF}}$	$\lambda_{\text{ITRF}}$	$h_{\text{ITRF}}$ (m)	Std ( $\phi$ ) [mm]	Std ( $\lambda$ ) [mm]	Std (h) [mm]
COL2	19°14'39.99520"N	103°42'06.78328"W	528.753	2	2	10
TNCC	18°47'27.89644"N	103°10'22.64093"W	1074.234	2	3	9
UCOE	19°48'47.44786"N	101°41'39.92204"W	1975.235	2	3	11
TECO	18°59'04.39521"N	103°51'39.67612"W	213.218	3	3	11
PENA	19°23'25.92280"N	104°06'05.31431"W	1490.975	2	3	10

northwest direction, Fig. 5(d). The movement at the last station (PENA) was mostly in the northwest and east directions, as shown in Fig. 5(e).

The GNSS observations of five IGS and UNAVCO stations' 3D displacement values are illustrated in Figs 4 and 6. The vertical displacement values of these five points are about 5–10 cm; see Fig. 4. The earthquake clearly caused significant changes in the horizontal coordinates on the Day of the Year 304 (Figs 5 and 6) (Pirtti *et al.* 2023).

It is confirmed by the time series of coordinate discrepancies from the IGS and UNAVCO GNSS stations

that there is a significant change of approximately 25 cm in the horizontal and of 10 cm in the height. On 19 September 2022, from 17:00 to 23:59:30 UTC Time, these horizontal discrepancies for TNCC and TECO stations change up to 25 cm (Pirtti *et al.* 2023).

With Synthetic Aperture Radarinterometry (InSAR), the epicentre of the earthquake and possible deformations can be determined. Whereas the GNSS gives a point-wise solution, the area deformation can be obtained from InSAR (Hooper *et al.* 2020; González *et al.* 2016; Lawrence *et al.* 2013). Thus, the verification of the effects determined by the

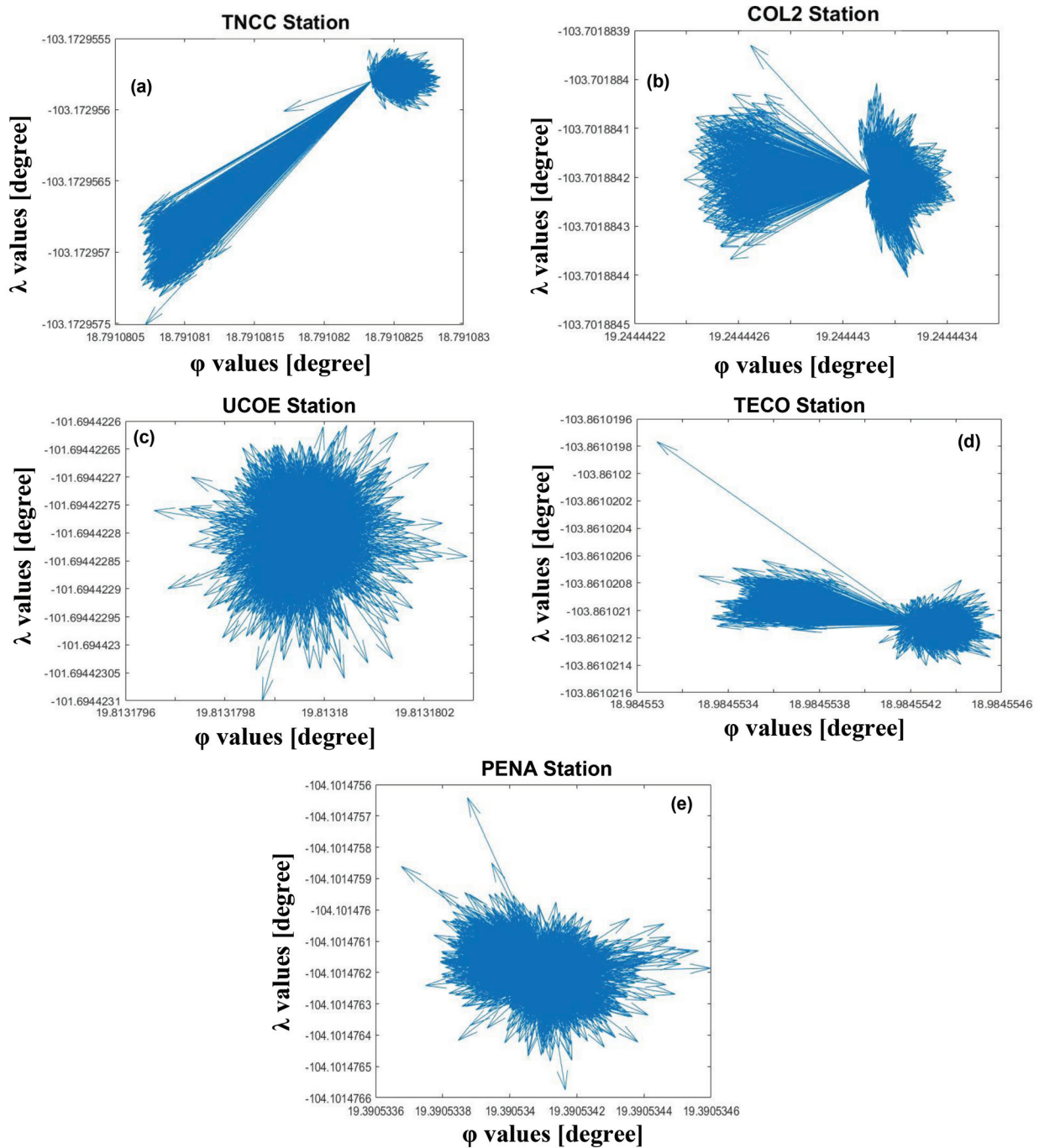


**Fig. 5** Earthquake-induced horizontal displacement vectors for five IGS and UNAVCO points on 19 September 2022 (00:00:00–23:59:30 UTC Time): (a) TNCC, (b) COL2, (c) UCOE, (d) TECO, (e) PENA



GNSS and other geodetic measurements is made by InSAR. The results obtained as a result of the kinematic GNSS evaluations made in this study were also compared with the InSAR images. By comparing the kinematic GNSS evaluations with InSAR images we can potentially improve the accuracy of the deformation measurements. Table 3 contains information about the data used.

LiCSAR Sentinel-1 is a platform that processes and provides InSAR data for users and is developed by COMET (Center for the Observation and Modelling of Earthquakes, Volcanoes and Tectonics) (Morishita *et al.* 2020). The interferograms presented in Table 3 were downloaded ready-made from the LiCSAR data archive and analysed. Figure 8 shows the earthquake epicentre along with the UCOE and

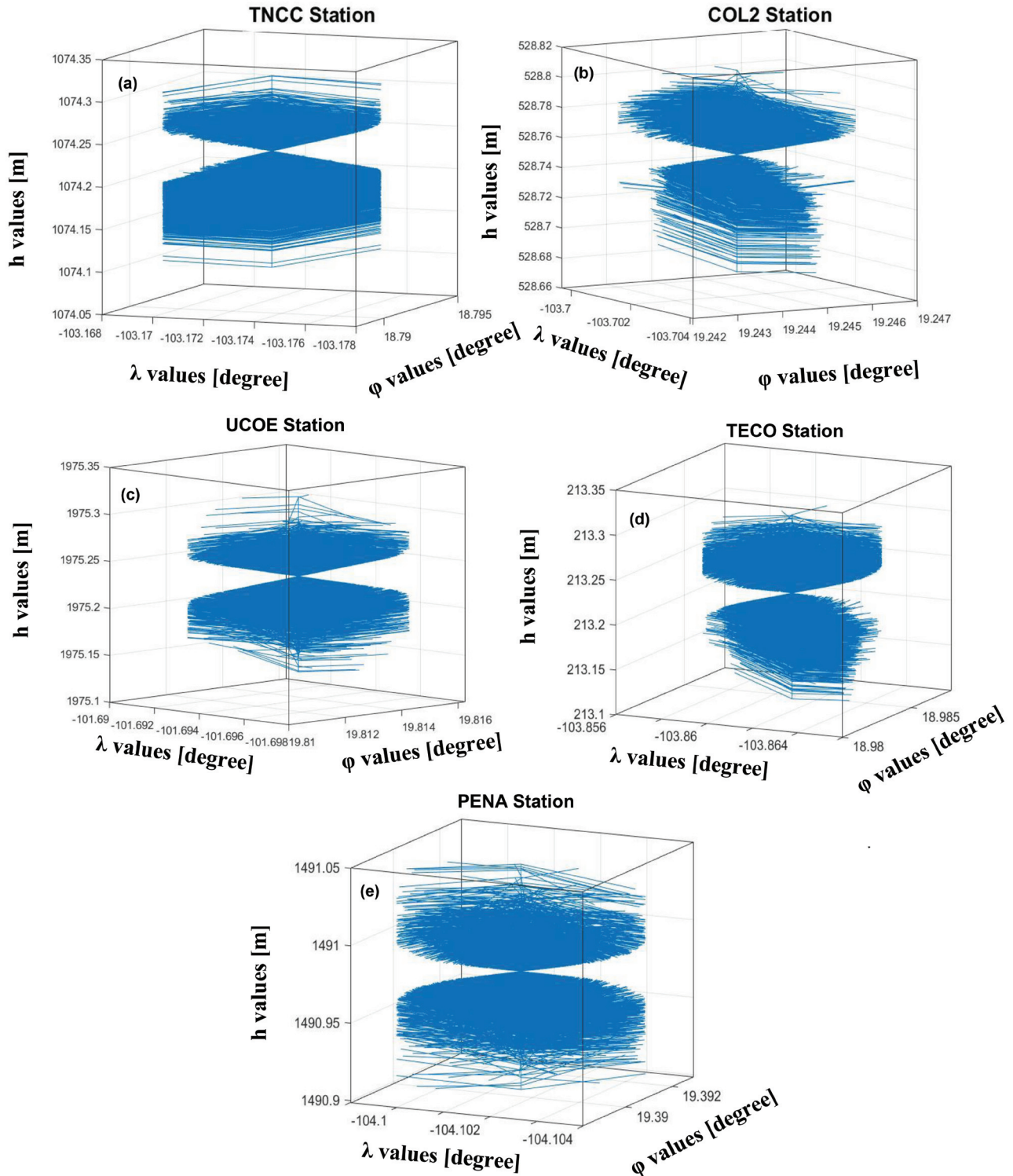


**Fig. 6** Mexico Michoacán earthquake-induced 3D displacement vectors for five IGS and UNAVCO points on 19 September 2022 (00:00:00–23:59:30 UTC Time)

**Table 3** Information of InSAR data

Satellite	Date	File type	Mode	Polarization	Relative orbit
Sentinel-1	6 September 2022	SLC	IW	VV	114
Sentinel-1	25 September 2022	SLC	IW	VV	114
Sentinel-1	6 September 2022	SLC	IW	VV	531
Sentinel-1	29 September 2022	SLC	IW	VV	531

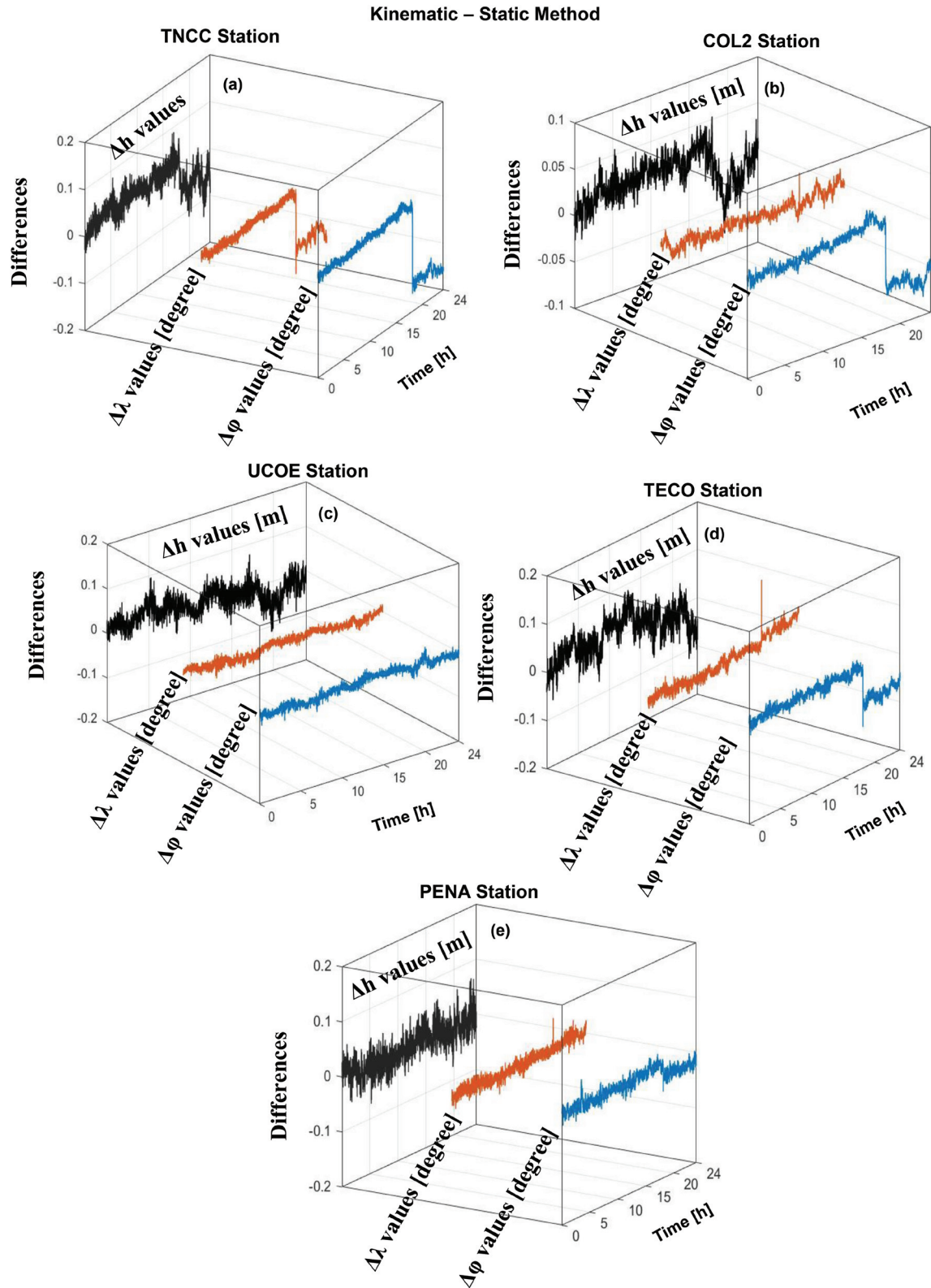


**Fig. 7** Comparison of all 3D locations of five IGS and UNAVCO IGS stations (including the outputs of static and kinematic analysis)



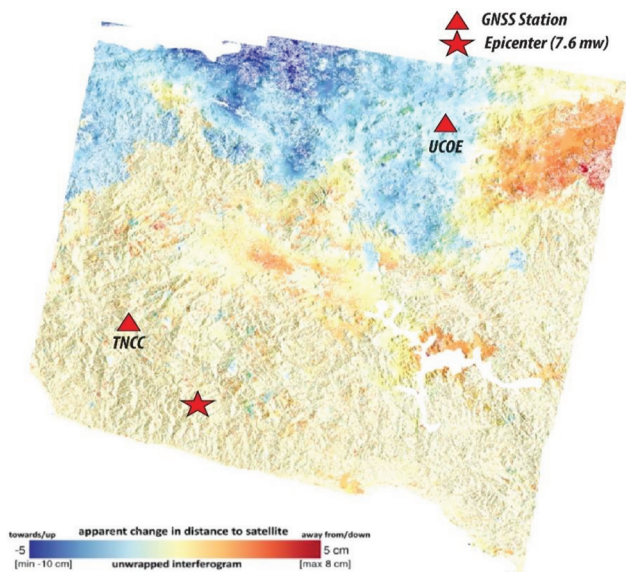


**Fig. 8** The epicentre of the earthquake (red star) and UCOE and TNCC stations with the interferogram

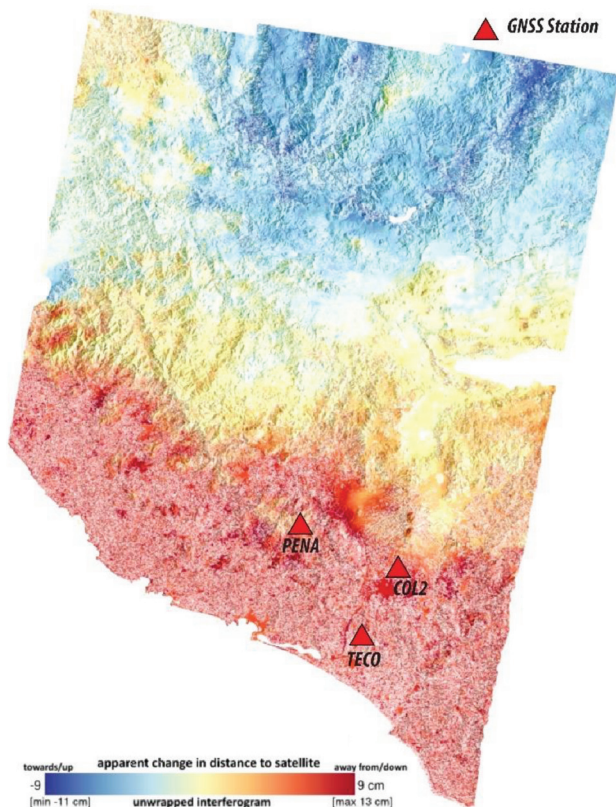


**Fig. 9** PENA, COL2 and TECO stations with the interferogram

TNCC GNSS stations on the interferogram. Similarly, Figure 9 includes the positions of the PENA, COL2, and TECO GNSS stations on the interferogram. The interferograms represent deformation in the unwrapped LOS (Line of Sight) direction. When compared with GNSS data, a high correlation (0.85) is observed in the earthquake-induced displacement

patterns. These maps visually demonstrate the coherence between the results obtained by the two methods, combining the point-specific accuracy of GNSS with the wide-area coverage of InSAR.

## CONCLUSIONS

The relative GNSS analysis method was used to successfully estimate the horizontal and vertical (co-seismic) displacements generated by the 19 September 2022 Michoacán – Mexico earthquake (Mw 7.6–7.7; 11:51:00 UTC time). For this, five stations in close proximity to the epicentre of the earthquake were chosen, so the data collected reflects the most relevant ground movements resulting from the seismic event. The daily GPS time series data was used to determine horizontal and vertical displacements with an accuracy of less than 1 mm. This level of accuracy is crucial for detecting subtle ground movements that can occur due to tectonic activity, volcanic processes, or other geophysical phenomena.

The results of displacement estimation are listed below:

- The maximum horizontal displacement value in the southwest direction was recorded by the TNCC station, which is located approximately 45 kilometres from the epicentre and northwest of the Michoacán-Colima fault.
- The TECO station, which is situated on the northwest side of the Michoacán-Colima fault and is around 70–80 km from the earthquake’s centre, recorded horizontal motions of 10–19 cm.

The horizontal displacement computed at other stations varies depending on their distance from the epicentre; however, it is smaller than that of the two previously mentioned stations (TNCC and TECO). The Michoacán-Colima earthquake causes a vertical displacement of 5–10 cm at five sites. The southwest, north, and west directions are more prevalent as movement directions at TNCC and TECO sites in this research. The deformations analysed and published by GNSS and COMET show similar patterns and were determined in accordance with the earthquake model.

## ACKNOWLEDGEMENT

LiCSAR includes Copernicus Sentinel data that have been processed and analyzed by the Centre for the Observation and Modelling of Earthquakes, Volcanoes, and Tectonics (COMET). LiCSAR utilizes JASMIN, the collaborative data analysis environment of the United Kingdom (<http://jasmin.ac.uk>). The authors are also grateful to the anonymous reviewers for their comments.

## REFERENCES

- Arámbula-Mendoza, R., Reyes-Dávila, G., Vargas-Bracamontes, D., González-Amezcuca, M., Navarro-Ochoa, C., Martínez-Fierros, A., Ramírez-Vázquez, A. 2018. Seismic monitoring of effusive-explosive activity and large lava dome collapses during 2013–2015 at Volcán de Colima, Mexico. *Journal of Volcanology and Geothermal Research* 351, 75–88. <https://doi.org/10.1016/j.jvolgeores.2017.12.017>
- Arroyo, D., García, D., Ordaz, M., Mora, A.M., Singh, S.K. 2010. Strong ground-motion relations for Mexican interplate earthquakes. *Journal of Seismology* 14, 769–785. <https://doi.org/10.1007/s10950-010-9200-0>
- Erkoç, M.H., Doğan, U. 2023. Datum definition for geodetic vertical velocity field derived from GNSS observations: a case study in western and southern Turkey. *Bulletin of Geophysics and Oceanography* 64(2), 135–148. <http://dx.doi.org/10.4430/bgo00412>
- Erkoç, M.H., Doğan, U., Yıldız, H., Sezen, E. 2022. Estimation of vertical land motion along the south and west coast of Turkey from multi-sensor observations. *Advances in Space Research* 70(7), 1761–1772. <https://doi.org/10.1016/j.asr.2022.06.022>
- Escobar, A. 2003. Desastres agrícolas en México. Catálogo histórico (CIESAS, Fondo de Cultura Económica, Mexico). Fondo de Cultura Económica; 1er edición, CIESAS, Mexico. [In Spanish].
- Galvis, F.A., Miranda, E., Heresi, P., Dávalos, H., Ruiz-García, J. 2020. Overview of collapsed buildings in Mexico City after the 19 September 2017 (Mw7.1) earthquake. *Earthquake Spectra* 36(S2), 83–109. <https://doi.org/10.1177/8755293020936694>
- García-Acosta, V. 2001. Los sismos en la historia de México. Fondo de Cultura Económica (FCE), CIESAS, UNAM, Mexico. [In Spanish].
- González, P.J., Walters, R.J., Hatton, E.L., Spaans, K., McDougall, A., Hooper, A.J., Wright, T.J. 2016. LiCSAR: Tools for automated generation of Sentinel-1 frame interferograms, AGU Fall Meeting, December 12–16, San Francisco, USA.
- Hooper, A., Juncu, D., McDougall, A., Walters, R.J., Watson, C., Weiss, J.R., Wright, T. 2020. LiCSAR: An Automatic InSAR Tool for Measuring and Monitoring Tectonic and Volcanic Activity. *Remote Sensing* 12(15), 2430. <http://dx.doi.org/10.3390/rs12152430>
- Lawrence, B.N., Bennett, V.L., Churchill, J., Jukes, M., Kershaw, P., Pascoe, S., Pepler, S., Pritchard, M., Stephens, A. 2013. Storing and manipulating environmental big data with JASMIN. *Proceedings of IEEE Big Data, October 6–9, 2013, San Francisco, USA*.
- Morishita, Y., Lazecky, M., Wright, T.J., Weiss, J.R., Elliott, J.R., Hooper, A. 2020. LiCSBAS: An Open-Source InSAR Time Series Analysis Package Integrated with the LiCSAR Automated Sentinel-1 InSAR Processor. *Remote Sensing* 12, 424. <https://doi.org/10.3390/rs12030424>
- Pırtı, A., Hoşbaşı, R.G., Yücel, M.A. 2023. Examination of the Earthquake (Samos Island) in Izmir (30. 10. 2020) by Using Cors-Tr GNSS Observations and InSAR Data. *KSCE Journal of Civil Engineering* 27, 135–144. <https://doi.org/10.1007/s12205-022-0392-y>
- Rodríguez-Pérez, Q., Márquez-Ramírez, V.H., Zúñiga, F.R. 2020. Seismicity characterization of oceanic earthquakes in the Mexican territory. *Solid Earth* 11, 791–806. <https://doi.org/10.5194/se-11-791-2020>
- Zúñiga, F.R., Valdés-González, C.M., Reyes, M.A. 2000. A general overview of the catalog of recent seismicity compiled by the Mexican Seismological Survey. *Geofísica Internacional* 39, 161–170.